

ARTICLE

Magnetic field-assisted photochemical oxidation of benzyl alcohol to corresponding aldehydes by introducing TiO₂(P25)-ZnO/Fe³⁺ as a novel nanophotocatalyst

Saied Fallahnezhad | Ali Amoozadeh

Department of Organic Chemistry,
Faculty of Chemistry, Semnan University,
Semnan, Iran

Correspondence

Ali Amoozadeh, Department of Organic
Chemistry, Faculty of Chemistry, Semnan
University, 35131-19111, Semnan, Iran.
Email: aamoozadeh@semnan.ac.ir

Funding information

Semnan University, Grant/Award
Number: Ali amoozadeh

Abstract

For the first time, the surface modification of nanophotocatalyst TiO₂(P25)-ZnO was reported by the introduction of Fe³⁺ for modulation of the photocatalytic activity. The nanophotocatalyst TiO₂(P25)-ZnO/Fe³⁺ was synthesized and its crystal structure, morphology, and photocatalytic activity were well determined by, diffuse reflectance spectroscopy, energy dispersive X-ray, X-ray diffraction, and scanning electron microscope analyses. The photocatalyst was applied for the selective oxidation of different aryl alcohols to the respective aldehyde beneath visible light (blue LED lamp, $\lambda > 420$ nm) in the presence of nitrate ion as oxidant. Also, for the first time, the effect of presence of an external magnetic field (5,000 G) contemporary with photoreaction was studied simultaneously by applying an external magnet field of 5,000 G and valuable results were obtained so that the time of photoreaction declined considerably up to 65%. This study has many advantages like the use of a magnetic field as a green technology, being clean, and zero energy. Also, the photoreaction did stop at the stage of aldehyde to provide a considerable selectivity.

KEYWORDS

magnetic field, photocatalyst, surface modification

1 | INTRODUCTION

The goal of TiO₂-based photocatalysts is to reduce organic contaminants.^[1–9] When a photon of enough high-energy encounters the surface of Titania, an electron (e[−]) can be banished from the valence band (VB) to the conduction band (CB). At the same time, this makes a hole (h⁺), which is the loss of an electron, in the VB. The holes can operate as forceful oxidizing agents, while the ejected electrons have powerful reducing ability. Because these two active kinds have a sufficiently long lifetime in semiconductor materials (such as TiO₂), their oxidizing and reducing power can operate on other species. TiO₂ has three crystalline phases: rutile, anatase,

and brookite. The anatase phase has superior photocatalytic attributes owing to the low recombination speed of electron–hole couples resulting from the devious bandgap. The band gaps of the rutile and anatase phase are 3.03 and 3.20 eV, severally, and blended rutile and anatase samples have greater work operation and electron affinities.^[10] Newly, the CB of anatase has been placed 0.2 eV under that of rutile.^[10] As considered in ref. [10], in the blended rutile and anatase samples, which have great photocatalytic activities, the electrons' motion from the rutile to the anatase phase, whenever the holes travel in the inverse orientation. Commercial Degussa TiO₂(P25) has a 3:1 combination proportion of anatase and rutile phases and a medium crystallite size of

21 nm.^[11] Although the manners for the adaptation of P25 are complicated and need high-temperature conditions.^[12] Also, the accurate mechanism and reason for the reclaimed photocatalytic attributes on correction are yet unfamiliar. However, the restriction of TiO₂ is its broad bandgap, which limited area from 3.0 to 3.2 eV, and can be only activated by ultraviolet (UV) light ($\lambda < 380$ nm). UV light comprises about 4% of the solar energy attaining at the Earth's surface.^[13] Because of the low entering flux, the photocatalytic activity of TiO₂ upon a broad span of wavelengths must be enhanced, and this has been the subject of many research studies. Zinc oxide is an inorganic compound with the formula ZnO. It is a white powder that is insoluble in water. ZnO is present in the Earth's crust as the mineral zincite, which crystallizes in three several structures: wurtzite, zinblende, and rock salt. ZnO has a powerful normal leaning to crystallize in the wurtzite structure and so, approximately all photocatalytic surveys are centralized on this structure. Pertaining on the optical absorption confidants, the refractive index of ZnO (2.0) is smaller than that of TiO₂ (2.5–2.7), so ZnO with difficulty diffuses light, thereupon manufacturing it colorless and improves the transparency.

Extensive research attempts have been managed toward raising the photocatalytic activity of TiO₂. The development of the TiO₂-based photocatalysts has accordingly appeared as a research subject of significance and immediacy.^[14] Expansion of new visible light-sensitive TiO₂ photocatalyst has been recently extensive through dye sensitization,^[15,16] transition metal,^[17] non-metal doping^[18,19] and surface modification.^[20,21] One method to come close to improving TiO₂ photocatalyst is to dope transition metals into TiO₂, and the other is to make coupled photocatalysts.^[14] It assists obtaining a longer electron lifetime by efficient charge separation.^[22] Although when the photocatalyst was blended, the decay was great as evaluated with the single catalyst.

There are many applications of metal-organic frameworks (MOFs) and MOF-derived materials that receive growing attention for fine chemical synthesis due to their versatile tunability and high catalytic activity.^[23] The selective oxidation with an active interface between Au-Pd alloy nanoparticles (NPs) and cobalt oxide supports via calcination of a composite of NPs encapsulated in MOFs was performed by Liao et al.^[24] Effectiveness of using a perovskite/Zr-MOFs heterojunction in realizing efficient and stable inverted p-i-n perovskite solar cells (PVSCs) is demonstrated by Lee et al.^[25] The MOFs and derivatives are used as catalysts for biomass conversion.^[26]

Imaginably, the surface affixation of TiO₂ with nanoclusters of, that is, Cu (II), Cr (III), Fe (III), and Ce

(III), was researched pending the last years.^[27–31] These matters suggest modified visible light sensibility via an interfacial charge transfer (IFCT) procedure without present extra impurity rates in the bandgap of the TiO₂. In electron transmission procedures, grafted transition metal nanoclusters can swiftly drop a quick photoinduced charge dissociation whenever lowering the charge transporter recombination speed owing to their significant action on as electron acceptors. Iron (Fe) has attracted intensive attention as a bone implant material because of its inherent biodegradability, favorable biocompatibility, and mechanical properties.^[32]

Nowadays, the application of magnetic nanocomposites as heterogeneous catalysts is a fascinating investigation zone. The surface functionalization of these matters is a tasteful route to bridge the split among heterogeneous and homogeneous catalyses.^[33] Whenever research on the efficacy of magnetic field on the solvent's confidants are comparatively scared, the efficacy of the magnetic field on the characteristic of water has been detected in the early 1900s by Danish Physicist Hendricks Anton Lorenz.^[34] This green technology is clean and has zero energy using up.^[35] The influence of the magnetic field on macroscopic features and microscopic structures of water has been formerly studied by Xiao-Feng and Bo.^[36] They have discovered several changes in the water confidants once imported to the magnetic field. The dynamic magnetization approach was carried out for the magnetization of water. Magnetic field-assisted arrangement of photocatalytic TiO₂ particles on membrane surface to enhance membrane antifouling for water treatment was the performance by Sun et al.^[37] and preparation of magnetic and photocatalytic membranes with improved performance by Liu et al.^[38]

Therefore, a nanocomposite of TiO₂ and ZnO (TiO₂-ZnO) has been prepared, surface was reclaimed with Fe(III) nanoclusters until TiO₂-P25-ZnO/Fe³⁺ was prepared and the surveying photochemical workmanship was researched. It is significant that the TiO₂-P25 which is protected by ZnO is developing the crowd of photosynthesized charge transporters owing to a synergistic interaction, whenever surface grafted Fe(III) ions partake in a poly-electron reduction procedure as well as suppressing the recombination of e⁻/h⁺ pairs. The redox potential of the Fe³⁺/Fe²⁺ redox pair (0.77 V vs. SHE, pH = 0) allows impressive IFCT procedures in this order. Then nanophotocatalyst was used in the oxidation of aryl alcohol to respective aldehydes and based on the literature,^[39] reduction of nitrate ion takes place via one of the several equations as a photocatalytic reaction. Then, in this research, we applied a magnetic field when a photocatalytic reaction was done, and was compared the presence and absence of magnetic field on the yield, photoreaction time and selectivity.

2 | EXPERIMENTAL

2.1 | Materials

All chemicals that were used in this research were bought by the Merck and Aldrich chemical companies with no requirement for extra purgation. $\text{TiO}_2(\text{P25})$ (ca. 70% anatase, 30% rutile; BET area ca. $50 \pm 15 \text{ m}^2 \text{ g}^{-1}$) powder was reserved by Degussa Company. Twice distilled water was applied for the procurement of different solutions. The pH of the solutions was co-equalled with 1 M HCl or 1 M NaOH. Progress of reactions was assayed by thin-layer chromatography on commercial sheets covered with silica gel and UV spectroscopy too. Fourier transform infrared spectroscopy (FT-IR) was performed on a Shimadzu FT-IR 8400 rig using Potassium Bromide pressed powder sheets in the span of $400\text{--}4,000 \text{ cm}^{-1}$. X-ray diffraction (XRD) was done for the $\text{TiO}_2(\text{P25})\text{-ZnO}/\text{Fe}^{3+}$ powder instance was conducted on a Siemens D5000 diffractometer (Siemens AG, Munich, Germany) using $\text{Cu-K}\alpha$ radiation of wavelength 1.54 \AA . Energy dispersive X-ray (EDX) spectra of the photocatalyst were attained by a Mira 3-XMU scanning electron microscope (SEM). The X-ray fluorescence (XRF, Model ARL PERFORMIX) was applied for the elemental analysis. Diffuse reflectance spectroscopy (DRS, Model Sinco S4100, Korea) was applied for the designation of the optical band split (Eg) of $\text{TiO}_2(\text{P25})\text{-ZnO}$ and $\text{TiO}_2(\text{P25})\text{-ZnO}/\text{Fe}^{3+}$. SEM images were obtained with a BAL-TEC SCD 005 SEM appliance operating at 10 kV. The reagents applied in this research were of analytical scale.

2.2 | Preparation of nanosized photocatalysts

2.2.1 | Nanosized heterostructured $\text{TiO}_2(\text{P25})\text{-ZnO}$ photocatalysts

$\text{TiO}_2(25)$ and $\text{Zn}(\text{NO}_3)_2 \cdot 6\text{H}_2\text{O}$ were applied as beginning materials, and NaOH was applied as the precipitant without major purification. $\text{Zn}(\text{NO}_3)_2 \cdot 6\text{H}_2\text{O}$ was dissolved in a least value of deionized water with fixed stirring up to a clear solution was caught and 1 M NaOH solution was augmented, white amorphous precipitates of $\text{Zn}(\text{OH})_2$ were obtained. The needed value of $\text{TiO}_2(\text{P25})$ was augmented with fixed stirring to the preparation of the hetero-structured $\text{TiO}_2(\text{P25})\text{-ZnO}$ photocatalysts with the Ti/zinc molar proportions of 10:1 holding pH 7. The precipitates were stirred for 20 hr for homogeneous mixing. The precipitates were filtered and

rinsed by deionized water to pick up the soluble ions. The humid powder received was dried at 100°C in the air to form the pioneers of the hetero-structured $\text{TiO}_2(\text{P25})\text{-ZnO}$ photocatalysts that were better calcinated at 250°C in air for 3 hr. The nanosized photocatalysts were collected in powder form labeled as $\text{Ti}_{10}\text{-Zn}$ (Ti/Zn molar ratios of 10:1).

2.2.2 | Surface affixation of the $\text{TiO}_2(\text{P25})\text{-ZnO}$ nanocomposites with Fe(III) ions ($\text{TiO}_2(\text{P25})\text{-ZnO}/\text{Fe}^{3+}$)

The affixation of Fe(III) nanoclusters on the surface of the synthesized $\text{TiO}_2(\text{P25})\text{-ZnO}$ composite was done by addendum, an easy impregnation manner that has been reported formerly.^[28] In summary, the suitable ratio (0.005–0.3 wt% Fe) of the iron salt was augmented into an aqueous $\text{TiO}_2\text{-P25-ZnO}$ suspension and stirred at 90°C for 1 hr for achieving Fe(III) nanoclusters on the surface $\text{TiO}_2(\text{P25})\text{-ZnO}$. Afterward, the aqueous solution was centrifuged three times after laundering with great values of distilled water and exsiccated at 110°C for 24 hr afore laborious the resulting solid into a nice powder that named $\text{Ti}_{10}\text{-Zn}/\text{Fe}^{3+}$.

3 | RESULTS AND DISCUSSION

In expanse of our continuous plans on procurement of new heterogeneous photocatalysts^[40] for organic reactions, we have proposed the procreation of nanophotocatalyst named $\text{TiO}_2(\text{P25})\text{-ZnO}/\text{Fe}^{3+}$ that was made of surface modification of $\text{TiO}_2(\text{P25})\text{-ZnO}$. This novel nanophotocatalyst was characterized via, XRD, EDX spectroscopy, DRS, and SEM. Nanophotocatalyst was used in the photoreaction with modification in terms of photoreaction. Then nanophotocatalyst was used in the oxidation of aryl alcohol to respective aldehydes as a photocatalytic reaction and was proofed the surface modification of nanocomposite, $\text{TiO}_2(\text{P25})\text{-ZnO}$ with Fe^{3+} , decreased the time of photoreaction so that, the time of photoreaction for $\text{TiO}_2(\text{P25})\text{-ZnO}$ was 5.5 h but, the time was decreased to 4 hr with $\text{TiO}_2(\text{P25})\text{-ZnO}/\text{Fe}^{3+}$. It is remarkable that the best prior time was 6 hr.^[40] Then, we applied a magnetic field (5,000 G), whereas with a photocatalytic reaction. The time of photoreaction decreased to 2 hr with $\text{TiO}_2(\text{P25})\text{-ZnO}/\text{Fe}^{3+}$. Also, selectivity of this photoreaction with photocatalyst was considerable. The photoreaction did stop at the stage of aldehyde and no acid was produced.

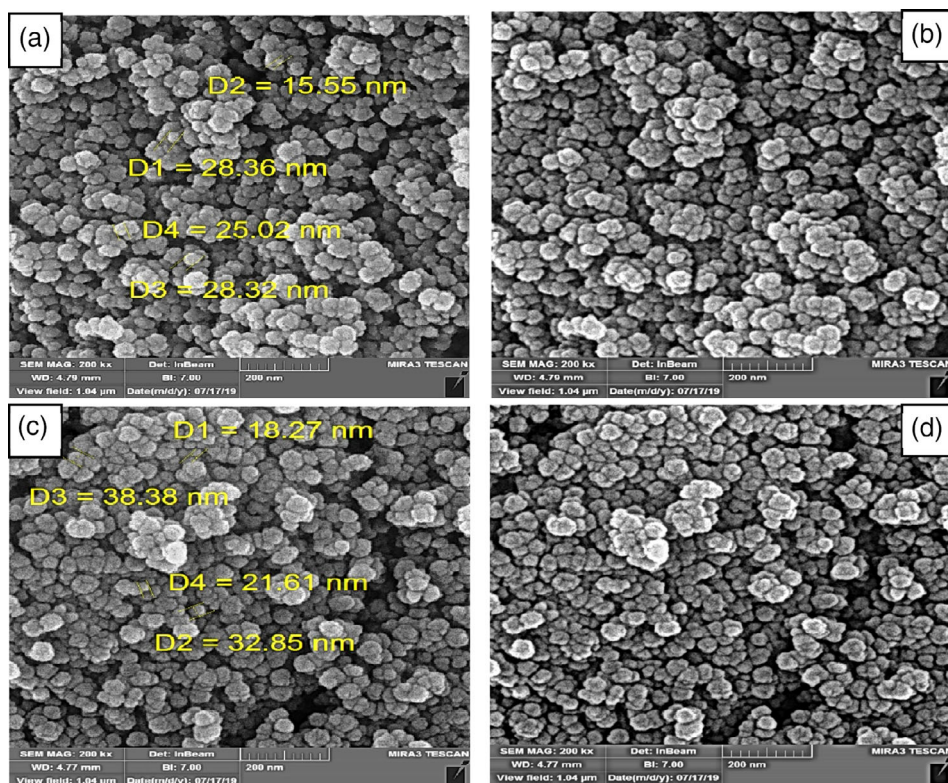


FIGURE 1 The FE-SEM images of (a, b) $\text{TiO}_2(\text{P25})\text{-ZnO}$ and (c, d) $\text{TiO}_2(\text{P25})\text{-ZnO}/\text{Fe}^{3+}$. (D: Particle Diagonal)

3.1 | Characterization of $\text{TiO}_2(\text{P25})\text{-ZnO}/\text{Fe}^{3+}$

3.1.1 | Field emission scanning electron microscopy

Field emission scanning electron microscopy (FE-SEM) is a famous and impressive gadget for perusal of the morphology of NPs. Conforming to the FE-SEM images of $\text{TiO}_2(\text{P25})\text{-ZnO}$ (Figure 1a,b), the middle measure of $\text{TiO}_2(\text{P25})\text{-ZnO}$ NP is within 15–30 nm. The FE-SEM images of $\text{TiO}_2(\text{P25})\text{-ZnO}/\text{Fe}^{3+}$ (Figure 1c,d) show the middle measure of $\text{TiO}_2(\text{P25})\text{-ZnO}/\text{Fe}^{3+}$ NP is within 18–30 nm. Spherical morphology can be proven of the FE-SEM images.

So, Scherrer equation calculation of photocatalyst proved that these particles were at nanoscale:

$$\beta = \frac{0.3198 * 3.14}{180} = 0.005578$$

$$D = K\lambda / (\beta * \text{Cos}\theta) = \frac{0.9 * 0.154}{0.005578 * \text{Cos} 12.67} = 25.469 \text{ nm}$$

3.1.2 | X-ray diffraction

XRD was made on crystals to study the phase sincerity and crystal structure of the nanophotocatalyst. The XRD

of nanophotocatalyst $\text{TiO}_2(\text{P25})\text{-ZnO}$ powder before surface modification and $\text{TiO}_2(\text{P25})\text{-ZnO}/\text{Fe}^{3+}$, after surface rectification are shown in (Figure 2). Alike summit severities of the $\text{TiO}_2(\text{P25})\text{-ZnO}$ and $\text{TiO}_2(\text{P25})\text{-ZnO}/\text{Fe}^{3+}$ indicate the consistency of the crystalline phase of nano- $\text{TiO}_2(\text{P25})$ pending preparation and surface rectification.

According to the XRD, the pattern of $\text{TiO}_2(\text{P25})$ was observed in all crystallograms. This shows that Fe^{3+} did not dope into the crystal structure. Because in this case, the XRD pattern of $\text{TiO}_2(\text{P25})$ would have changed. Of course, high energy (such as laser) is required for doping, which is not provided (in our case) by mixing, blending, or sonicating. Also, based on the literatures^[41,42] in these cases, ESR spectroscopy at 77 k had been reported that (Fe^{3+}) species were grafted onto the crystal surface as

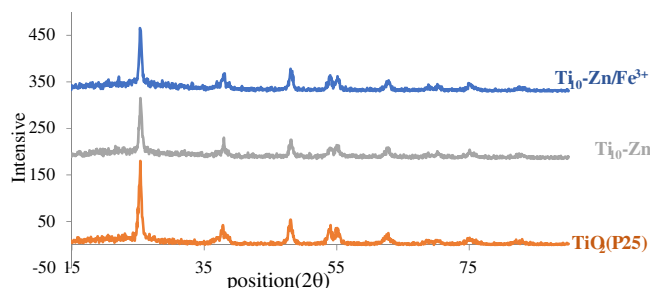


FIGURE 2 The XRD image of $\text{TiO}_2(\text{P25})$, $\text{TiO}_2(\text{P25})\text{-ZnO}$, and $\text{TiO}_2(\text{P25})\text{-ZnO}/\text{Fe}^{3+}$

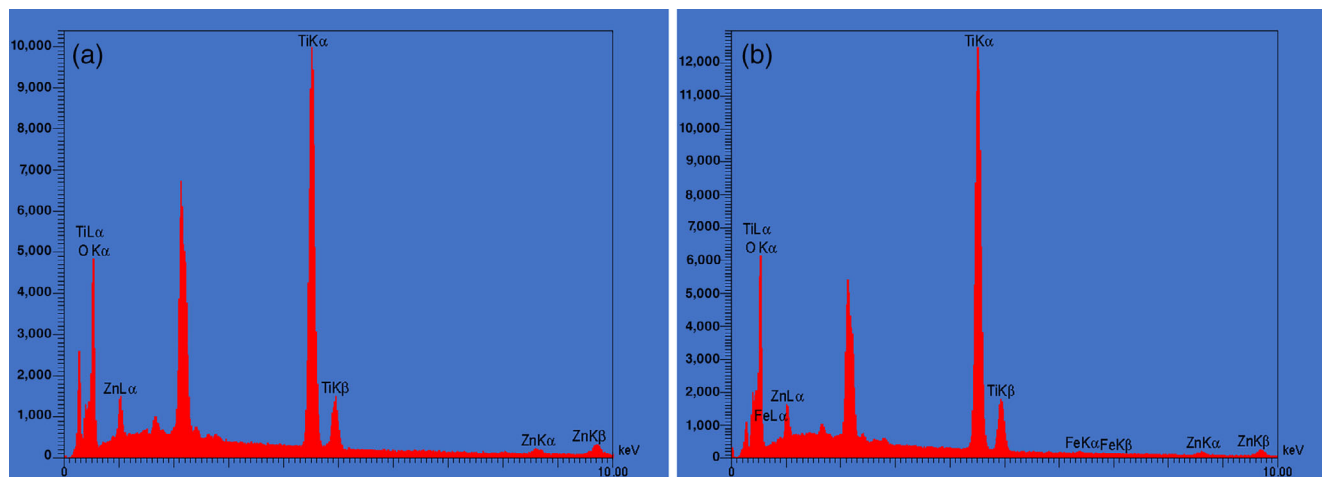


FIGURE 3 The EDX patterns of the (a) $\text{TiO}_2(\text{P25})\text{-ZnO}$ and (b) $\text{TiO}_2(\text{P25})\text{-ZnO/Fe}^{3+}$

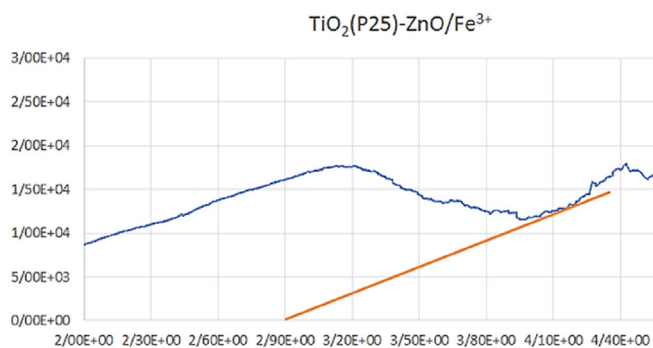


FIGURE 4 Bandgap of $\text{TiO}_2\text{-P25@ZnO/Fe}^{3+}$

amorphous with distorted structure and Fe^{3+} was not doped into the crystal structure of $\text{TiO}_2(\text{P25})$.

3.1.3 | Energy-dispersive X-ray spectroscopy

EDX spectroscopy as a useful interpretive method was done for the elemental analysis or chemical description of NPs. The EDX analysis displays the entity of oxygen, titanium, and Zinc in the nanophotocatalyst $\text{TiO}_2(\text{P25})\text{-ZnO}$, (Figure 4a). The EDX analysis proved the presence of Fe in $\text{TiO}_2(\text{P25})\text{-ZnO}$ addition to NPs of $\text{TiO}_2(\text{P25})\text{-ZnO}$ as well (Figure 3b).

3.1.4 | Diffuse reflectance spectroscopy

The band split energies of $\text{TiO}_2(\text{P25})\text{-ZnO}$ were improved with Fe^{3+} as shown in Figure 4. As shown in Figure 4, the band gap energy of these photocatalysts, $\text{TiO}_2(\text{P25})\text{-ZnO/Fe}^{3+}$ is 2.9 eV. So, it is obvious that a significant decrease on band split energy and red shift occur by

surface modification on the $\text{TiO}_2(\text{P25})$. Accordingly, photo-activity of $\text{TiO}_2(\text{P25})\text{-ZnO/Fe}^{3+}$ would gain growth visible wavelength.

3.1.5 | Recyclability

Recycling experiments. As responsiveness, increase about environmental concerns, industries are looking for ways to remove their pollution. This is where the recycling and reusability of catalysts matter. So, the catalyst is required to have wonderful catalytic activity and selectivity. Also, actual stability during the cycles. Accordingly, the reusability of $\text{TiO}_2(\text{P25})\text{-ZnO/Fe}^{3+}$ was examined. As shown in Figure 5, the catalyst was capable of performing six consecutive runs, without significant loss of activity.

3.2 | Evaluation of the photocatalytic activity

The photo-activity of photocatalyst was appraised by photocatalytic oxidation of aryl alcohol beneath visible light radiancy. The photocatalytic oxidation of aryl alcohol tests was done in a 15 ml Pyrex glass armed with a water whirling jacket to rein the temperature of reactions. Photo-reactor was fixed at room temperature during the experiments. Dummy radiation into the Pyrex reactor was prepared via 4×3 W blue light-evolving diode lamps as the visible light origin. Photocatalyst was suspended in 5 ml acetonitrile, benzyl alcohol (150 μmol) as reductant, and sodium nitrate (150 μmol) was added as oxidant. Results were monitored with UV spectroscopy. Benzyl alcohol produced benzaldehyde. So, we followed increasing the absorbance of UV-Vis spectra related the benzaldehyde had produced, until the

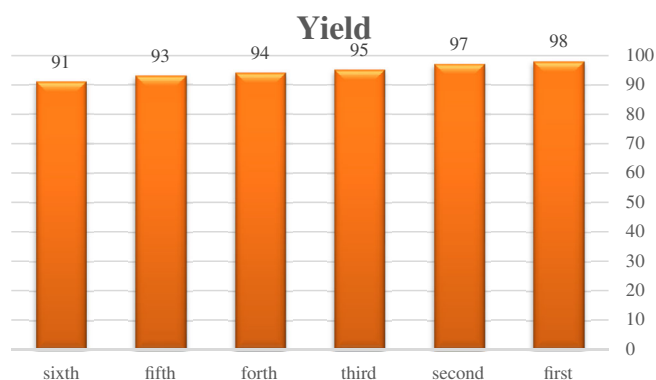


FIGURE 5 Recyclability of $\text{TiO}_2(\text{P25})\text{-ZnO/Fe}^{3+}$ on the oxidation of benzyl alcohol to corresponding aldehydes

absorbance was stopped. This means that benzaldehyde production was completed. Of course, we monitored benzaldehyde production with TLC monitoring. The results were the same.

For comparison of the effect of surface modification with Fe^{3+} , at first, was done the photoreaction with $\text{TiO}_2(\text{P25})\text{-ZnO}$. The time of photoreaction was 5.5 hr.

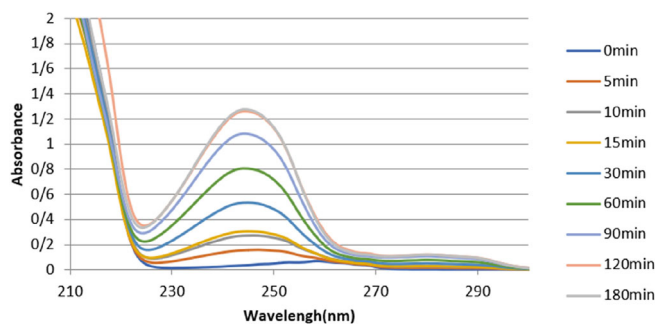


FIGURE 6 The emission spectrum of the blue LED lamp and UV-Vis absorption spectrum of $\text{TiO}_2(\text{P25})\text{-ZnO/Fe}^{3+}$

Then $\text{TiO}_2(\text{P25})\text{-ZnO/Fe}^{3+}$ was used and the time decreased to 4 hr.

Then we designed photoreaction in the magnetic field. Therefore, a magnetic field 5,000 G prepared. Two magnets ($4\text{ cm} \times 4\text{ cm} \times 5\text{ cm}$) 5,000 G with 3 cm space between them were fixed in two holes of Teflon fixture. The results were considerable and remarkable. The time of photoreaction decreased to 2.5 hr with $\text{TiO}_2(\text{P25})\text{-ZnO/Fe}^{3+}$.

TABLE 1 Reaction conditions: magnetic field 5,000 G, $3 \times 4\text{w}$ LED blue lamp, sodium nitrate as a solvent

Entry	Reactant	Photocatalyst	Product	Time
1		$\text{TiO}_2(\text{P25})\text{-ZnO/Fe}^{3+}$		120 min
2		$\text{TiO}_2(\text{P25})\text{-ZnO/Fe}^{3+}$		120 min
3		$\text{TiO}_2(\text{P25})\text{-ZnO/Fe}^{3+}$		120 min
4		$\text{TiO}_2(\text{P25})\text{-ZnO/Fe}^{3+}$		20 hr
5		$\text{TiO}_2(\text{P25})\text{-ZnO/Fe}^{3+}$		20 hr

TABLE 2 The comparison of reaction efficiency for different catalytic systems under the optimized conditions

Entry	Catalyst	Light source	Time (hr)	Yield ^a /Sel. (%)
1	TiO ₂ (P25)-ZnO/Fe ³⁺	Blue LED	2	100/100
1	<i>n</i> -TiO ₂ -P25-SO ₃ H ^[40]	Blue LED	7	99/99
2	<i>n</i> -TiO ₂ -P25@ECH@WO ₃ -SO ₃ H ^[39]	Blue LED	6	99/99
3	<i>n</i> -TiO ₂ -P25@ECH@WO ₃	Blue LED	6	20/99
4	<i>n</i> -TiO ₂ -P25@ECH@ZnO	Blue LED	6	10/99
5	<i>n</i> -TiO ₂ -P25@ECH@ZrO ₂ -SO ₃ H	Blue LED	6	55/99
6	<i>n</i> -TiO ₂ -P25@ECH@ZrO ₂	Blue LED	6	Trace/99
7	TiO ₂ -P25@TDI@DES ^[41]	Blue LED	19	70/78
8	TiO ₂ /Ag ^[42]	Blue LED	4	88/88

Note: Reaction conditions: benzyl alcohol (150 μmol), NaNO₃ (150 μmol), acetonitrile (5 ml), N₂ atmosphere, room temperature, and 4 × 3 W LED irradiation.
^aYield was determined by UV/Vis spectroscopy.

The results were very good. The efficacy of the magnetic field on the progress of photoreaction was interesting and valuable. Then, our research group modified the amount of photocatalyst in the reaction performed by the magnetic field. Finally, the best amount of photocatalyst (0.1 g) was determined. The results were phenomenal. Modified amount of photocatalyst is different in the attendance or absence of a magnetic field. The emission spectrum of the blue LED lamp and UV-Vis absorption spectrum of TiO₂(P25)-ZnO/Fe³⁺ proved that the photoreaction was completed for 120 min. Remarkable that the best prior time was 6 hr. Figure 6.

Finally, derivatives of benzyl alcohol were used as reductant and following results were observed (Table 1).

3.3 | Comparison of the characteristic of new synthesized catalyst with some reported catalysts

In Table 2, entry 1 (new synthesized catalyst) was compared with some reported photocatalyst.

4 | CONCLUSIONS

For the first time, TiO₂-P25-ZnO/Fe³⁺ has been synthesized as a new photocatalyst by the surface modification of TiO₂(P25)-ZnO with Fe³⁺. The prepared photocatalyst was well specified by XRD, DRS, EDX, and SEM analyses. The XRD introduced the crystallinity preservation of nano-TiO₂-P25-ZnO/Fe³⁺. SEM outcomes certified nanometer-sized particles of the photocatalyst and the attendance of Ti, Zn, Fe and, O atoms was proved in the EDX spectrum. Photocatalyst was used for the electric photocatalytic oxidation of aryl alcohols to the

respective aldehydes below visible light irradiation in entity of nitrate ion. Also, for the first time, such photoreaction was performed in the presence of an external magnetic field (5,000 G) and excellent yield and valuable results were observed. Also, the time of the photoreaction decreased up to 65% comparing the same conditions without external applied magnetic field. The use of external magnetic field is a green technology and clean and has zero energy using up. This manner has some valuable benefits such as useful easiness, great photocatalytic performance, moderate reaction situation, easy work-up without purification with column chromatography, environmentally friendly, and reusability of the photocatalyst for several continuous cycles with stable activity.

ACKNOWLEDGMENTS

The authors appreciatively thank the faculty of the chemistry of Semnan University, for suffering this research.

REFERENCES

- [1] J. Mahy, V. Cerfontaine, D. Poelman, F. Devred, E. Gaigneaux, B. Heinrichs, S. Lambert, *Materials* **2018**, *11*, 584.
- [2] Q. Tian, W. Wei, J. Dai, Q. Sun, J. Zhuang, Y. Zheng, P. Liu, M. Fan, L. Chen, *Appl. Catal., B* **2019**, *244*, 45.
- [3] M. Pelaez, N. T. Nolan, S. C. Pillai, M. K. Seery, P. Falaras, A. G. Kontos, P. S. Dunlop, J. W. Hamilton, J. A. Byrne, K. O'shea, *Appl. Catal., B* **2012**, *125*, 331.
- [4] G. L.-M. Léonard, C. A. Pàez, A. E. Ramírez, J. G. Mahy, B. Heinrichs, *J. Photochem. Photobiol., A* **2018**, *350*, 32.
- [5] J. J. Reinos, C. M. Á. Docio, V. Z. Ramírez, J. F. F. Lozano, *Ceram. Int.* **2018**, *44*, 2827.
- [6] K. Kasinathan, J. Kennedy, M. Elayaperumal, M. Henini, M. Malik, *Sci. Rep.* **2016**, *6*, 38064.
- [7] J. G. Mahy, S. D. Lambert, R. G. Tilkin, C. Wolfs, D. Poelman, F. Devred, E. M. Gaigneaux, S. Douven, *Mater. Today Energy* **2019**, *13*, 312.

- [8] C. Byrne, L. Moran, D. Hermosilla, N. Merayo, Á. Blanco, S. Rhatigan, S. Hinder, P. Ganguly, M. Nolan, S. C. Pillai, *Appl. Catal., B* **2019**, 246, 266.
- [9] Q. Li, T. Zhao, M. Li, W. Li, B. Yang, D. Qin, K. Lv, X. Wang, L. Wu, X. Wu, *Appl. Catal., B* **2019**, 249, 1.
- [10] D. O. Scanlon, C. W. Dunnill, J. Buckeridge, S. A. Shevlin, A. J. Logsdail, S. M. Woodley, C. R. A. Catlow, M. J. Powell, R. G. Palgrave, I. P. Parkin, *Nat. Mater.* **2013**, 12, 798.
- [11] T. C. Jagadale, S. P. Takale, R. S. Sonawane, H. M. Joshi, S. I. Patil, B. B. Kale, S. B. Ogale, *J. Phys. Chem. C* **2008**, 112, 14595.
- [12] M. Wang, B. Nie, K.-K. Yee, H. Bian, C. Lee, H. K. Lee, B. Zheng, J. Lu, L. Luo, Y. Y. Li, *Chem. Commun.* **2016**, 52(14), 2988.
- [13] G. Yang, Z. Jiang, H. Shi, T. Xiao, Z. Yan, *J. Mater. Chem.* **2010**, 20, 5301.
- [14] P. Bansal, P. Kaur, D. Sud, *Desal. Water Treat.* **2014**, 52, 7004.
- [15] H. Kato, A. Kudo, *J. Phys. Chem. B* **2002**, 106(19), 5029.
- [16] A. L. Linsebigler, G. Lu, J. T. Yates Jr., *Chem. Rev.* **1995**, 95, 735.
- [17] Y. Ma, X. Wang, Y. Jia, X. Chen, H. Han, C. Li, *Chem. Rev.* **2014**, 114(19), 9987.
- [18] T. Ohno, T. Mitsui, M. Matsumura, *Chem. Lett.* **2003**, 32, 364.
- [19] B. O'regan, M. Grätzel, *Nature* **1991**, 353, 737.
- [20] S. Sato, *Chem. Phys. Lett.* **1986**, 123(1-2), 126.
- [21] X. Wang, R. Yu, P. Wang, F. Chen, H. Yu, *Appl. Surf. Sci.* **2015**, 351, 66.
- [22] N. V. N. Mai, D. T. Lim, N. Q. Bac, N. T. H. Chi, D. T. Dung, N. N. Pham, D. N. Nhiem, *J. Chin. Chem. Soc.* **2020**, 67, 242.
- [23] H. Konnerth, B. M. Matsagar, S. S. Chen, M. H. Pechtl, F.-K. Shieh, K. C.-W. Wu, *Coord. Chem. Rev.* **2020**, 416, 213319.
- [24] Y.-T. Liao, N. Ishiguro, A. P. Young, C.-K. Tsung, K. C.-W. Wu, *Appl. Catal., B* **2020**, 270, 118805.
- [25] C. C. Lee, C. I. Chen, Y. T. Liao, K. C. W. Wu, C. C. Chueh, *Adv. Sci.* **2019**, 6, 1801715.
- [26] R. Fang, A. Dhakshinamoorthy, Y. Li, H. Garcia, *Chem. Soc. Rev.* **2020**, 49(11), 3638.
- [27] Y. Nosaka, S. Takahashi, H. Sakamoto, A. Y. Nosaka, *J. Phys. Chem. C* **2011**, 115, 21283.
- [28] X. Qiu, M. Miyauchi, H. Yu, H. Irie, K. Hashimoto, *J. Am. Chem. Soc.* **2010**, 132, 15259.
- [29] H. Irie, S. Miura, R. Nakamura, K. Hashimoto, *Chem. Lett.* **2008**, 37, 252.
- [30] H. Irie, K. Kamiya, T. Shibamura, S. Miura, D. A. Tryk, T. Yokoyama, K. Hashimoto, *J. Phys. Chem. C* **2009**, 113, 10761.
- [31] R. Nakamura, A. Okamoto, H. Osawa, H. Irie, K. Hashimoto, *J. Am. Chem. Soc.* **2007**, 129, 9596.
- [32] C. Shuai, Y. Li, F. Deng, Y. Yang, S. Peng, F. Qi, L. Shen, *Appl. Sci.* **2020**, 10, 2487.
- [33] C. S. Gill, B. A. Price, C. W. Jones, *J. Catal.* **2007**, 251(1), 145.
- [34] R. Gehr, Z. A. Zhai, J. A. Finch, S. R. Rao, *Water Res.* **1995**, 29, 933.
- [35] M. Bakherad, A. Keivanloo, Z. Bakherad, Z. Toozandejani, M. Mahdavi, *J. Chin. Chem. Soc.* **2019**, 66, 674.
- [36] X.-F. Pang, B. Deng, *Phys. B* **2008**, 403(19-20), 3571.
- [37] T. Sun, Y. Liu, L. Shen, Y. Xu, R. Li, L. Huang, H. Lin, *J. Colloid Interface Sci.* **2020**, 570, 273.
- [38] Y. Liu, L. Shen, H. Lin, W. Yu, Y. Xu, R. Li, T. Sun, Y. He, *J. Membr. Sci.* **2020**, 612, 118378.
- [39] M. Bitaraf, A. Amoozadeh, *Res. Chem. Intermed.* **2021**, 1, 3329.
- [40] S. Hosseini, A. Amoozadeh, *J. Photochem. Photobiol., A* **2018**, 364, 516.
- [41] S. Taghavi, A. Amoozadeh, F. Nemat, *J. Chem. Technol. Biotechnol.* **2021**, 96, 384.
- [42] T. Shamsi, A. Amoozadeh, *Appl. Organomet. Chem.* **2021**, 35, e6276.

How to cite this article: S. Fallahnezhad, A. Amoozadeh, *J. Chin. Chem. Soc.* **2021**, 1, <https://doi.org/10.1002/jccs.202100300>